

Dynamics of a bricklayer model: Multi-walker realizations of true self-avoiding motion

A. C. Maggs

UMR 7083 Gulliver, ESPCI Paris, PSL University, 10 rue Vauquelin,
Paris, 75005, France.

Contributing authors: anthony.maggs@espci.fr;

Abstract

We investigate a multi-walker generalization of the true self-avoiding walk, formulated as a bricklayer model where agents collectively build a growing interface. We investigate the coupled partial differential equations that describe the hydrodynamic limit of this process. Stochastic simulations of N walkers confirm these analytic predictions in the large- N limit, revealing a characteristic parabolic density profile. These results provide a continuum description for the dynamics of non-reversible Monte Carlo algorithms, offering insights into the relaxation mechanisms of collective sampling schemes.

Orcid: [0000-0002-9071-5063](https://orcid.org/0000-0002-9071-5063)

Keywords: True self-avoiding walk, non-reversible Monte Carlo, Event-chain simulation

Introduction

The true self-avoiding walk [1] was introduced to describe a growing polymer on a lattice, where the monomer to be added to the end of the walk tries to avoid previously visited sites. During the growth process the probability of choosing a site i , which has already been visited $h_i(t)$ times is then

$$p_i(t+1) = \frac{e^{-\lambda h_i(t)}}{\sum_j e^{-\lambda h_j(t)}} \quad (1)$$

The sum is over all neighbors j of the current position at time t . $\lambda > 0$ is the strength of the repelling interaction. The large-scale behavior of the process is believed to be independent of λ , up to rescaling in space and time. The model was studied using approximate analytic tools, and it was concluded that the statistics of this walk are distinct from those of an equilibrium polymer [1, 2]. This self-avoiding process has found applications in several fields, including repelling chemotaxis [3, 4]. Great progress in understanding this process was made in a series of papers [5–8], which give the full analytic solution to the motion in one spatial dimension. In particular, it was demonstrated that the motion explores a spatial extent growing in time as $t^{2/3}$. These papers give explicit results for the distribution function of the end-to-end separation of the walk.

Our interest in this model arises from the fortuitous discovery [9] that the dynamics of the true self-avoiding walk are identical to the large-scale dynamics of a family of non-reversible Monte Carlo algorithms, the Event Chain Monte Carlo algorithm, ECMC, [10–12] when applied to a simple harmonic chain [13] or particles interacting with a Lennard-Jones potential [14]. In two dimensions such non-reversible algorithms have been exceptionally powerful in the study of hexatic transitions [15, 16]. We would like to understand this success by studying the large scale motion and relaxation of non-reversible algorithms: We note that the mode structure of molecular dynamics (applied to a simple fluid) reproduces the Navier-Stokes equations, from which one deduces the relaxation of fluctuations near equilibrium via the propagation of density, momentum and energy modes. A mapping of the dynamics of ECMC to a set of partial differential equations will allow us to study the relaxation of non-reversible algorithms firstly in one dimension, but through obvious generalizations in higher dimensions too.

The founding paper [1] of this model also studied the process in the continuum with the coupled equations

$$\frac{dX(t)}{dt} = -\frac{\partial h(X(t), t)}{\partial x}, \quad (2)$$

$$\frac{\partial h(x, t)}{\partial t} = \delta(x - X(t)). \quad (3)$$

In eq. (2) the function $h(x, t)$, the continuum version of h_j counts visits to the position $X(t)$, which now acts as a repulsive potential in the motion. The end position of the polymer relaxes by gradient descent in a potential $h(x)$. In eq. (3) the repulsive potential is itself modified by the walker's visits to the position $X(t)$. We note that we have changed notation compared to older papers, including our own, to remain consistent with [17], the main inspiration of the present paper.

Eq. (2) can be interpreted as the motion of a particle moving at velocity $u = -\partial h(t, X(t))/\partial x$. If we now generalize to N independent particles with $\rho(x) = \sum_{i=1}^N \delta(x - X_i(t))$, with each particle moving at speed u_i eq. (2) implies a continuity equation of the form

$$\frac{\partial \rho}{\partial t} + \frac{\partial(u\rho)}{\partial x} = 0, \quad (4)$$

This continuity equation for mass is standard in continuum mechanics and hydrodynamics with a velocity field u . Each of the N independent walkers contributes to the

collective repulsive motion; we take spatial derivative ($\partial/\partial x$) of eq. (3) to find

$$\frac{\partial u}{\partial t} + \frac{\partial \rho}{\partial x} = 0. \quad (5)$$

The properties of the coupled hyperbolic equations (4, 5) for a collection of many walkers are the main subject of the present paper. We are particularly interested in such a many walker generalization of the true self-avoiding walk since it informs us as to the large scale dynamics of a parallel implementation of ECMC [18] where multiple agents or processors update a physical system. Many properties of the partial differential equations eq. (4,5) are established in [17], where these equations are shown to be the continuum limit of a discrete model, which the authors interpret as a company of N bricklayers building a long wall. To build a uniform wall, masons preferentially move down the local gradient of height h , leaving one brick on the wall each time they move. One is led to consider the collective hydrodynamic behavior of N independent bricklayers described by a continuum density distribution, $\rho(x)$, as a natural generalization of the true self-avoiding walk. Note there is a small but significant difference between the original true self-avoiding walk of [1], and that of [5, 17]. The first counts visits to lattice sites, the second counts the traversal of links between two sites. One hopes, and indeed it has been recently demonstrated that the large-scale motions of the models are the same [8] when $N = 1$.

Non-reversible Monte Carlo methods have direct analogies in discrete lattice models [11]; ECMC applied to hard-sphere systems always moves particles forwards in a manner which is familiar from the “totally symmetric simple exclusion process”, (TASEP). Non-reversible, forwards Monte Carlo [19] is thus in the same universality class as TASEP, and can thus be mapped onto both the noisy Burgers equation and the KPZ equation. The observation of the link between ECMC (for harmonic chains) and the true self-avoiding walk has also motivated the introduction of a lifted TASEP [20–22] which has been studied by Bethe diagonalization; it has direct analogies with the discreet construction of the true self-avoiding motion in the appendix of [5].

Below, we define the discrete model of bricklayers and perform simulations on this model with a variable number of bricklayers, N . We consider the analytic solution of the partial differential equations for the case of bricklayers all starting on the same lattice site. We also study the dynamics of bricklayers starting at random positions on a periodic, circular wall.

Bricklayers

Let us recall, briefly, the discrete model of [17]. A wall is being built with bricks added on the links $j, j + 1$ of a one-dimensional lattice. The number of bricks on this link is denoted h_j . Inspired by the continuum equations, we also introduce the discrete negative gradient of h_j such that $z_j = h_{j-1} - h_j$. The bricklayers are on the nodes of the lattice with no constraints on their occupation number. The number of bricklayers at site j is n_j . At any moment a single bricklayer can jump to the right or left, leaving one brick in the appropriate link. Jumps of each bricklayer occur at a rate $r(z_j)$,

distributed according to a Poisson process. One imposes

$$r(z)r(-z+1) = 1, \quad (6)$$

so that the local jump rate depends on the local gradient of the wall's height, corresponding to the number of previous visits of bricklayers. In our numerical work, we choose $r \sim \exp(\beta z)$ with $\beta = 0.4$. When a bricklayer jumps, the following changes of configuration may occur:

$$(n_j, z_j), (n_{j+1}, z_{j+1}) \rightarrow (n_j - 1, z_j - 1), (n_{j+1} + 1, z_{j+1} + 1)$$

with rate $n_j r(z_j)$, since any one of the n_j bricklayers can move, and

$$(n_j, z_j), (n_{j-1}, z_{j-1}) \rightarrow (n_j - 1, z_j + 1), (n_{j-1} + 1, z_{j-1} - 1)$$

with rate $n_j r(-z_j)$.

Both $\sum_j n_j = N$ and $\sum_j z_j$ are conserved, as is the parity of $(n_j + z_j)$ for each site. In the long-time limit, we expect to generate smooth distribution functions. It is natural to identify the discrete label j and the continuum variable x . The discrete occupation number n_j maps to the distribution $\rho(x)$ and z_j is linked to $u(x)$. We generate a starting configuration and store the randomly generated event times using the C++ `multiset` container. Use of the `multiset` data structure allows one to find and update events with a complexity which increases only logarithmically with the system size. We find the time of the first event, update the configuration, and recalculate times for sites that have been modified. The process is repeated to evolve the system a total time t requiring the simulation of $O(tN)$ events.

Scaling with number of bricklayers

We consider a simple generalization of previously given scaling arguments [2, 23] for the width of the function ρ after time t , starting with all builders on a single site. We consider a system with N builders, with a characteristic spatial scale which is given by $\ell \sim N^\beta t^\alpha$ at time t . The number of events is comparable to Nt , which builds a wall of height Nt/ℓ . The gradient of height must then scale as $\partial h/\partial x \sim Nt/\ell^2$. After acting for a time t on the bricklayers, this must give motion again comparable to $N^\beta t^\alpha = Nt^2/(N^{2\beta} t^{2\alpha})$. This implies $\alpha = 2/3$, $\beta = 1/3$, so that the extent of the distribution varies as

$$\ell \sim N^{1/3} t^{2/3}.$$

The mean density in the occupied region then varies as $(N/t)^{2/3}$. We find in our simulations that these results hold when $t \gg N$ so that the mean occupation of bricklayers is smaller than unity. We estimate that the time to explore a system of length L scales as $t \sim L^{3/2}/N^{1/2}$. See Fig. 1 for confirmation of these scaling laws.

Simulation results

We performed simulations to study the evolution of the functions $h(x, t)$ and $\rho(x, t)$. We place all the bricklayers on a single starting site (the origin $x = 0$ in our figures)

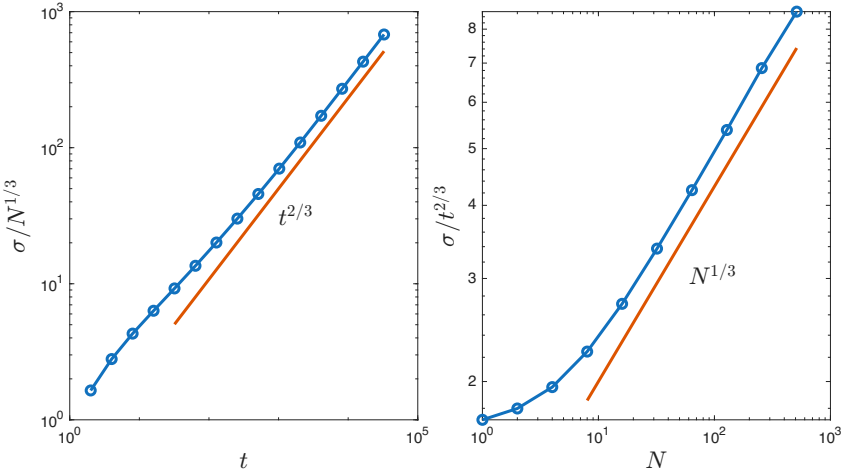


Fig. 1: Left: $N=256$, variance, σ , of distribution $\rho(x)$ as a function of time. Right: $t = 8000$, variance, σ , of $\rho(x)$ as a function of N . Data from 10^6 realizations.

and at the end of the simulation record the empirical distributions. To generate high-quality data, we typically average over 10^6 realizations of the process. The number of realizations that we use is large enough that the statistical errors are smaller than the linewidth of the curves that we plot. The data for different times and numbers of bricklayers display disparate scales; when we compare the distribution functions, we scale the functions to unit area and unit variance (by scaling the abscissa by the variance, σ), and denote the result $\bar{\rho}(\bar{x}, t)$ and $\bar{h}(\bar{x}, t)$, with scaled coordinate \bar{x} and scaled distributions $\bar{\rho}$ and \bar{h} . All simulations are performed on a periodic system, which is at least 16 times larger than the largest variance of ρ observed in the simulations. The system size is thus effectively infinite.

We studied the case $N = 1$ for which explicit results are known analytically [7], confirming that the function $\bar{\rho}(\bar{x}, t)$ is correctly reproduced by the simulations. See $N = 1$ in Fig. 2a. We then varied the number of bricklayers while keeping the simulation time constant at $t = 512$. The double-peak structure familiar from $N = 1$ is maintained, but the peaks are pushed to larger (scaled) separations; the distribution of density drops to zero more abruptly for large values of N . The evolution of \bar{h} is shown in Fig. 2b: For small N , the average wall height has a sharp maximum at the origin (the site where the builders were placed), but this is replaced by a broad maximum for N large.

We also studied the evolution in time when starting with $N = 512$ bricklayers, Fig. 3. At short times, $t = 2$ there is a peak at the origin, corresponding to builders that have not yet had time to move. By time $t = 4$ a dip has formed in the distribution function. The dip is shallower for the longest time shown, $t = 512$.

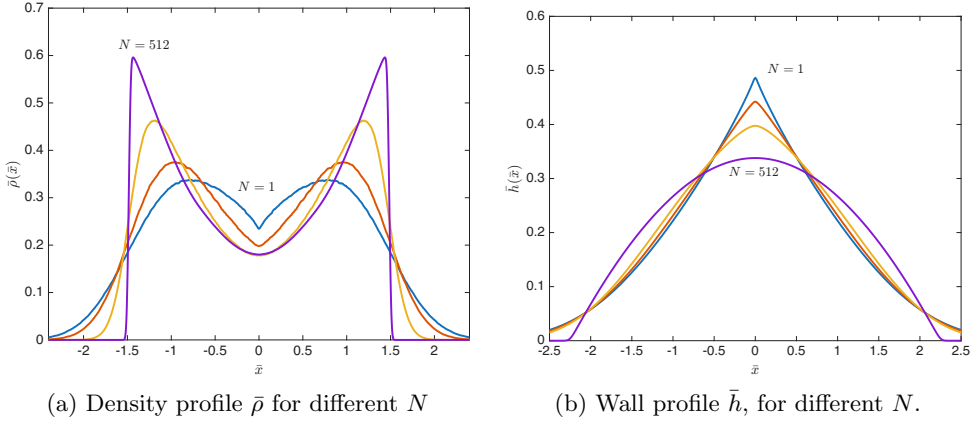


Fig. 2: Evolution of the density of builders $\bar{\rho}(\bar{x})$ and wall shape $\bar{h}(\bar{x})$ with builder number $N = 1, 4, 16, 512$ for fixed time $t = 8192$. Curves scaled to unit area and unit variance for comparison. The case $N = 1$ reproduces the known distribution of the true self-avoiding walk. Curves averaged over 10^6 realizations.

Scaling solution of partial differential equations

Scaling analysis tells us that the coupled partial differential equations have a solution of the form

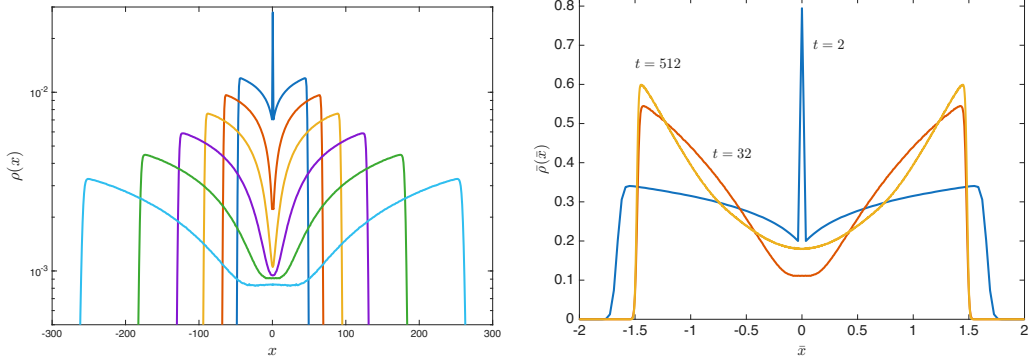
$$\begin{aligned}\rho &= \frac{1}{t^{2/3}} f(x/t^{2/3}), \\ u &= \frac{1}{t^{1/3}} g(x/t^{2/3}).\end{aligned}$$

These scaling relations are similar to those displayed by the solution to the KPZ equation. Substituting into the partial differential equations, we find coupled equations of f and for g which we write in matrix form:

$$\begin{pmatrix} 3g - 2y & 3f \\ 3 & -2y \end{pmatrix} \begin{pmatrix} f' \\ g' \end{pmatrix} = \begin{pmatrix} 2f \\ g \end{pmatrix}, \quad (7)$$

where $y = x/t^{2/3}$. Clearly, there is a trivial solution to these equations: $f(y) = g(y) = 0$.

We used a Runge-Kutta integrator to solve eq. (7) from initial values of f and g at $y = 0$. The value of $f(0)$ can be chosen to be unity by a rescaling of x and t , and the natural choice for a non-singular odd function g is $g(0) = 0$. In Fig. 4 we show the numerical solution of the coupled equations. We find that to high accuracy $g(y)$ is a linear function of y , while $f(y)$ is quadratic. These results are surprising, since for large y both functions must be zero; they describe the finite time evolution of a compact distribution of bricklayers. We show below that this is possible if we introduce



(a) Evolution of the density $\rho(x)$, for times $t = 2, t = 4, t = 8, t = 16, t = 32, t = 64$. Logarithmic scale. The width increases with t .

(b) Evolution of the density $\bar{\rho}(\bar{x})$, for times $t = 2, t = 32, t = 512$. Curves scaled to unit variance.

Fig. 3: Distribution functions for different times for $N = 512$. For the shortest time a peak of density remains at the origin. This peak rapidly disappears, leaving a central depression in the density distribution. At the longest time the density approaches an asymptotic parabolic form, with a rapid fall to zero at finite \bar{x} . Data from 10^6 realizations.

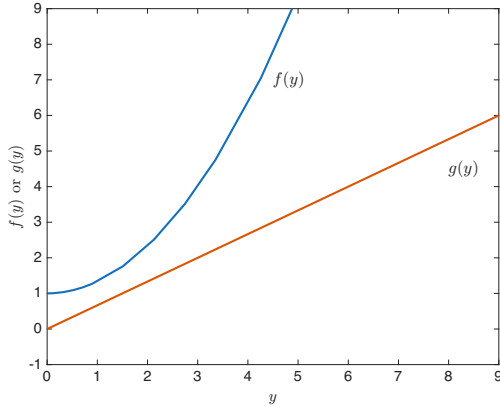


Fig. 4: Integration of the coupled equations eq. (7), starting from $f(0) = 1$ and $g(0) = 0$. The functions $f(y)$ and $g(y)$ do not decrease to zero for large y .

discontinuities in the two functions, so that the solution jumps to the trivial solution $f(y) = g(y) = 0$.

Analytic solution of the differential equations

The theory of hyperbolic partial differential equations (PDE) is complicated by the non-uniqueness of solutions in the presence of shocks or discontinuities. The theory

of the selection of the correct physical solution in such cases is subtle and will not be attempted here. We rather construct a solution from observation of the simulation data Fig. 3, informed by the numerical integration of the coupled equations Fig. 4. Empirically, we understand that the long-time limit of the function ρ is parabolic as found by the numerical integration, but it is truncated to zero at some finite $y = y_0$, as shown by the simulations. Such discontinuous, weak, solutions are ubiquitous in the theory of hyperbolic PDEs.

From the numerical integration for the scaling functions, we see that $g = \gamma y$. If we choose $3\gamma = 2$ the equations are simple, and we only need to solve

$$3f' = 2yg' + g \quad (8)$$

for f giving $f = A + y^2/3$. Let a discontinuity occur at $y = y_0$, then balancing the singularities in eq. (8) gives $3\Delta f - 2y_0\Delta g = 0$, where Δf and Δg are the jumps in the respective functions. This allows us to relate A and y_0 giving $A = y_0^2/9$. We also have that the total number of bricklayers is given by

$$\int_{-y_0}^{y_0} f(y) dy = 2y_0 A + 2y_0^3/9 = N \quad (9)$$

so

$$y_0 = \left(\frac{9N}{4} \right)^{1/3}, \quad (10)$$

agreeing with the previous scaling argument for the width of the distribution as a function of N . We integrate $g(y)$ to find the wall profile: we have $-\partial h/\partial x = (1/t^{1/3})(2/3)(x/t^{2/3}) = 2x/(3t)$ so that $h(x, t) = B - \frac{1}{3}x^2/t$ with the zero of h at $x = t^{2/3}y_0$. Thus, $B = (1/3)t^{1/3}y_0^2$. The scaling form of the solution to the partial differential equations is

$$h(x, t) = \frac{t^{1/3}}{3} \left(y_0^2 - \left(\frac{x}{t^{2/3}} \right)^2 \right) \Theta(y_0 - |x/t^{2/3}|), \quad (11)$$

$$\rho(x, t) = \frac{1}{9t^{2/3}} \left(y_0^2 + 3 \left(\frac{x}{t^{2/3}} \right)^2 \right) \Theta(y_0 - |x/t^{2/3}|), \quad (12)$$

$$u(x, t) = \frac{2x}{3t} \Theta(y_0 - |x/t^{2/3}|). \quad (13)$$

The equations display discontinuous behavior at $|x/t^{2/3}| = y_0$.

In Fig. 5 we plot the evolution of the empirical distribution ρ as a function of the number of bricklayers N plotting as a function of \bar{x}^2 . For these detailed comparisons, we use up to $N = 1024$ bricklayers, with simulation times up to $t = 32, 384$ to ensure the convergence of the distribution functions. We see that simulations with N large converge to a triangular function in this plot, indicating that the empirical distribution $\rho(x)$ is parabolic at large times.

From our data, it is also possible to measure the width of the transition region from large to small ρ . An empirical fit finds this width $w \sim t^{2/3}/N^{0.4}$. This is larger

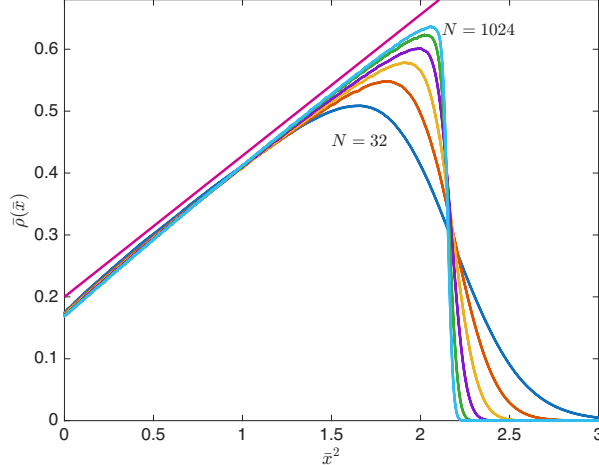


Fig. 5: Density distributions for $N=32, 64, 128, 256, 512, 1024$. Plotted on a quadratic scale to show convergence of the distributions to triangular form as N increases. Straight line guide for the eye. This plot implies that the final scaling function $f(y)$ is a simple quadratic function for large N and $t \gg N$. t up to 32, 384. Data from 10^6 realizations.

than the mean spacing between builders, $t^{2/3}/N^{2/3}$ when $N \gg 1$. We note, however, that the control of systematic and statistical errors is difficult for this sub-leading quantity, and are unable to give errors bounds on this estimated fit. In addition, this law is produced as an average over many samples. It is not clear to what degree this scaling reflects inter-sample variation, rather than the density gradient within a single realization. We have been unable to find an explanation for this law, which goes beyond the continuum limit of the partial differential equations. In the context of TASEP the density profile near shocks and discontinuities has generated a substantial and rich mathematical literature [24].

Linearized equations

When there are many bricklayers distributed along the wall, and the slope of the wall is small, we write $\rho = \rho_0 + \tilde{\rho}$ finding the linearized equation for the density field,

$$\frac{\partial^2 \tilde{\rho}}{\partial t^2} = \rho_0 \frac{\partial^2 \tilde{\rho}}{\partial x^2}. \quad (14)$$

This is a wave equation with propagation speed $c^2 = \rho_0$. The bricklayers move in traveling waves when they are dense. We perform simulations by randomly placing pairs of builders (to impose even parity on (z_j+n_j)) on $L/8$ sites of a flat wall of L sites, imposing periodic boundary conditions; we simulate sufficient time to come to a steady state, then record the longest wavelength Fourier components of ρ . We calculate $P(t) = c(t)^2 + s(t)^2$, with $c(t) = \sum_j n_j \cos(qj)$ and $s(t) = \sum_j n_j \sin(qj)$ for $q = 2\pi/L$. For a single traveling wave $P(t)$ is constant. In the presence of two counter-rotating waves

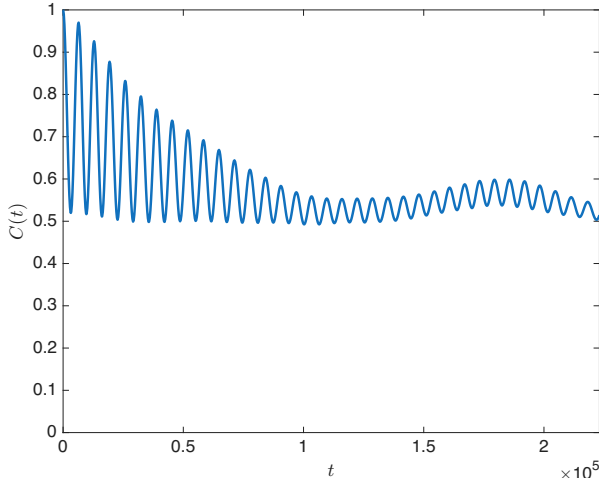


Fig. 6: Simulation of a periodic system of $L = 8192$ sites. $L/4$ bricklayers are placed in pairs, on random sites. The normalized autocorrelation, $C(t)$ of $P(t)$ displays oscillations. Data from a single simulation of length $t = 3 \times 10^6$

on a ring there are moments of constructive and destructive interference. In Fig. 6 we plot the autocorrelation of P and observe coherent oscillations. On longer time scales, the amplitude of the oscillations is modulated, nonlinearities in the equations give rise to amplitude exchange between modes. In this very long simulation wrap around of propagating waves occurs on the time scale of the oscillations.

Conclusions

We have found a (possibly non-unique) analytic solution to the partial differential equation describing a generalized multi-walker true self-avoiding motion. This solution is compatible with numerical simulations of the model of [17] in the large N and large t limit. Both the interface profile h and the bricklayer density ρ are simple quadratic functions of the position, but are truncated at some finite distance. The builders, trying individually to fill in low-lying segments of the wall, self-organize into a quadratic density of extent $t^{2/3}N^{1/3}$ with the maximum in density occurring at the edges of the new wall.

The true self-avoiding walk has been shown to have application in describing the dynamics of non-reversible Monte Carlo simulations: Bricklayers are analogous to “active particles” in these methods, the wall height corresponds to the displacement of atoms by the algorithm. A parallel multi-agent version version of this algorithm has been described in [18]. It will be interesting to see if the ideas of the present paper can also be applied to such non-reversible Monte Carlo algorithms in two or more dimensions with multiple agents. In many implementations of non-reversible Monte Carlo, the active particle is resampled at regular intervals in order to improve the ergodicity

of the method, this corresponds to additional source and sink terms in eq. (4)

$$\frac{\partial \rho}{\partial t} + \frac{\partial(u\rho)}{\partial x} = \lambda - \mu\rho, \quad (15)$$

where λ is the creation rate of new builders, and μ a death rate. Such a generalized wave equation has a tuneable damping which can be used to suppress wave propagation. We note also that with certain parameter values, non-reversible Monte Carlo generates oscillating states, where the convergence of thermodynamic averages becomes difficult to control. The oscillating states found in our simulations of the bricklayer model are perhaps linked to this point.

Acknowledgments. The author thanks W. Krauth for discussions on the formulation of lifted TASEP.

Declarations

- Competing Interests: The author has no competing or financial interest in this paper.
- Funding: No funds, grants, or other support was received.
- Code availability: <https://github.com/acmaggs/Avoid/tree/main/Bricks>.
- The author performed all planning, coding and data analysis.

References

- [1] Amit, D.J., Parisi, G., Peliti, L.: Asymptotic behavior of the "true" self-avoiding walk. Phys. Rev. B **27**, 1635–1645 (1983) <https://doi.org/10.1103/PhysRevB.27.1635>
- [2] Pietronero, L.: Critical dimensionality and exponent of the "true" self-avoiding walk. Phys. Rev. B **27**, 5887–5889 (1983) <https://doi.org/10.1103/PhysRevB.27.5887>
- [3] d'Alessandro, J., Barbier-Chebbah, A., Cellerin, V., Benichou, O., Mège, R., Voituriez, R., Ladoux, B.: Cell migration guided by long-lived spatial memory. Nature Communications **12**(1), 4118 (2021) <https://doi.org/10.1038/s41467-021-24249-8>
- [4] Barbier-Chebbah, A., Bénichou, O., Voituriez, R.: Self-interacting random walks: Aging, exploration, and first-passage times. Phys. Rev. X **12**, 011052 (2022) <https://doi.org/10.1103/PhysRevX.12.011052>
- [5] Tóth, B.: The "True" Self-Avoiding Walk with Bond Repulsion on \mathbb{Z} : Limit Theorems. The Annals of Probability **23**(4), 1523–1556 (1995) <https://doi.org/10.1214/aop/1176987793>
- [6] Tóth, B., Werner, W.: The true self-repelling motion. Probability Theory and Related Fields **111**(3), 375–452 (1998) <https://doi.org/10.1007/s004400050172>

- [7] Dumaz, L., Tóth, B.: Marginal densities of the "true" self-repelling motion. *Stochastic Processes and their Applications* **123**(4), 1454–1471 (2013) <https://doi.org/10.1016/j.spa.2012.11.011>
- [8] Kosygina, E., Peterson, J.: Convergence of rescaled "true" self-avoiding walks to the Tóth-Werner "true" self-repelling motion (2025). <https://arxiv.org/abs/2502.10960>
- [9] Maggs, A.C.: Non-reversible Monte Carlo: An example of "true" self-repelling motion. *Europhysics Letters* **147**(2), 21001 (2024) <https://doi.org/10.1209/0295-5075/ad64ff>
- [10] Bernard, E.P., Krauth, W., Wilson, D.B.: Event-chain Monte Carlo algorithms for hard-sphere systems. *Phys. Rev. E* **80**, 056704 (2009) <https://doi.org/10.1103/PhysRevE.80.056704>
- [11] Kapfer, S.C., Krauth, W.: Irreversible local Markov chains with rapid convergence towards equilibrium. *Phys. Rev. Lett.* **119**, 240603 (2017) <https://doi.org/10.1103/PhysRevLett.119.240603>
- [12] Michel, M., Kapfer, S.C., Krauth, W.: Generalized event-chain Monte Carlo: Constructing rejection-free global-balance algorithms from infinitesimal steps. *The Journal of Chemical Physics* **140**(5), 054116 (2014) <https://doi.org/10.1063/1.4863991>
- [13] Eberle, A., Lörlер, F.: Convergence rates of self-repellent random walks, their local time and Event Chain Monte Carlo (2025). <https://arxiv.org/abs/2511.23453>
- [14] Maggs, A.C.: Event-chain Monte Carlo and the true self-avoiding walk. *Phys. Rev. E* **111**, 054104 (2025) <https://doi.org/10.1103/PhysRevE.111.054104>
- [15] Kapfer, S.C., Krauth, W.: Two-dimensional melting: From liquid-hexatic coexistence to continuous transitions. *Phys. Rev. Lett.* **114**, 035702 (2015) <https://doi.org/10.1103/PhysRevLett.114.035702>
- [16] Lei, Z., Krauth, W.: Irreversible Markov chains in spin models: Topological excitations. *Europhysics Letters* **121**(1), 10008 (2018) <https://doi.org/10.1209/0295-5075/121/10008>
- [17] Tóth, B., Werner, W.: In: Sidoravicius, V. (ed.) *Hydrodynamic Equation for a Deposition Model*, pp. 227–248. Birkhäuser Boston, Boston, MA (2002). https://doi.org/10.1007/978-1-4612-0063-5_9 . https://doi.org/10.1007/978-1-4612-0063-5_9
- [18] Li, B., Todo, S., Maggs, A.C., Krauth, W.: Multithreaded event-chain Monte Carlo with local times. *Computer Physics Communications* **261**, 107702 (2021) <https://doi.org/10.1016/j.cpc.2020.107702>

- [19] Lei, Z., Krauth, W.: Mixing and perfect sampling in one-dimensional particle systems. *Europhysics Letters* **124**(2), 20003 (2018) <https://doi.org/10.1209/0295-5075/124/20003>
- [20] Lei, Z., Krauth, W., Maggs, A.C.: Event-chain Monte Carlo with factor fields. *Phys. Rev. E* **99**, 043301 (2019) <https://doi.org/10.1103/PhysRevE.99.043301>
- [21] Essler, F.H.L., Krauth, W.: Lifted TASEP: A solvable paradigm for speeding up many-particle Markov chains. *Phys. Rev. X* **14**, 041035 (2024) <https://doi.org/10.1103/PhysRevX.14.041035>
- [22] Massoulié, B., Erignoux, C., Toninelli, C., Krauth, W.: Velocity trapping in the lifted totally asymmetric simple exclusion process and the true self-avoiding random walk. *Phys. Rev. Lett.* **135**, 127102 (2025) <https://doi.org/10.1103/mqdr-x95j>
- [23] Ottinger, H.C.: A short note on the true self-avoiding walk. *Journal of Physics A: Mathematical and General* **18**(6), 299 (1985) <https://doi.org/10.1088/0305-4470/18/6/007>
- [24] Ferrari, P.L., Ghosal, P., Nejjar, P.: Limit law of a second class particle in TASEP with non-random initial condition. *Annales de l'Institut Henri Poincaré, Probabilités et Statistiques* **55**(3), 1203–1225 (2019) <https://doi.org/10.1214/18-AIHP916>